scribed pressure gradient (e.g., at $f = 40$ Hz and $A = 0.1\%$; see Fig. 2), the wake component could not be fitted with the universal function W, while the "law-of-the-wall" still applied. The wake component is, therefore, more strongly affected by the imposed oscillations than is the wall component.

Ensemble-averaged velocities phase locked to the oscillations indicate that a large fraction of the fluctuations are correlated to the motion of the flap and are coherent across the boundary layer. The amplitudes and the relative phases of the fundamental (forced) frequency suggest that the external excitation generates an array of spanwise vortices extending across the entire boundary layer. Fourier analysis of the phase-locked data reveals that the maximum value of the fundamental frequency and its first harmonic at a given location decreases rapidly with increasing X. The maximum value of the subharmonic content of the signal remains approximately constant with increasing X, and dominates the flow at large distances from the flap. The emergence of the subharmonic as the dominant frequency is correlated with dH/dX being positive.

One may conclude by restating that the introduction of harmonic, two-dimensional oscillations results in a reattachment of the flow and changes the proportions between the "wake" and the "wall" functions whose linear combination represents the streamwise velocity distribution in a turbulent boundary layer. It does not, however, alter the universal form of these functions.

ACKNOWLEDGMENT

This work is supported in part by AFOSR Grant No. 86-0323.

[a] Present address: Department of Aerospace and Mechanical Engineering, University of Arizona, Tucson, Arizona 85721.

[1] D. Neuburger and I. Wygnanski, in *Proceedings of the AFOSR Workshop on Unsteady Separated Flow*, F. J. Seiler Research Labs-TR88-0004, 1987.
[2] D. Oster, I. Wygnanski, B. Dziomba, and H. Fiedler, in *Lecture Notes in Physics*, edited by H. Fiedler (Springer, Berlin, 1978), Vol. 75, p. 48.
[3] G. L. Brown and A. Roshko, J. Fluid Mech. **64**, 775 (1974).
[4] M. Gaster, E. Kit, and I. Wygnanski, J. Fluid Mech. **150**, 23 (1985).
[5] D. Coles, J. Fluid Mech. **1**, 191 (1956).

Filamentation of unstable vortex structures via separatrix crossing: A quantitative estimate of onset time

L. M. Polvani[a] and G. R. Flierl
Center for Meteorology and Physical Oceanography, Massachusetts Institute of Technology, Cambridge, Massachusetts 02139

N. J. Zabusky[b]
Department of Mathematics and Statistics, University of Pittsburgh, Pittsburgh, Pennsylvania 15260

(Received 25 August 1988; accepted 25 October 1988)

The onset of filamentation for compact vortex structures in two-dimensional incompressible flows is elucidated. An estimate is presented for the filamentation time of an unstably perturbed Kirchhoff ellipse, obtained from a linear analysis of the geometry of the instantaneous corotating streamfunction.

The filamentation of compact vortex structures in two-dimensional (2-D) incompressible flows is being recognized as a dominant mechanism for enstrophy cascade and is associated with their chaotic evolutions. Melander *et al.*[1] showed that the geometrical patterns of critical (stagnation) points and separatrices of a proper, comoving streamfunction yield insight into the relative flow of vorticity. Deem and Zabusky[2] were the first to observe very fine filaments emerging from a strongly perturbed piecewise constant stable vortex (Kirchhoff) ellipse and Dritschel[3] found a remarkable repeated filamentation of a weakly perturbed Rankine (circular) vortex at long times.

In this Letter, we present concepts and quantitative results for simple cases that relate the onset of filamentation to the time, t_C, when perturbed vortex contours cross the separatrices emanating from hyperbolic points in the comoving streamfunction. In contrast with previous work,[3–5] where amplification was due to nonlinear interactions, we examine in detail *linearly* unstable harmonic perturbations[6] and the filamentation of Kirchhoff ellipses. Calculating the geometry of the comoving streamfunction and the contour, we obtain an analytic estimate for t_C based on linear theory. At that time the hyperbolic points of the comoving streamfunction penetrate the vortex contour, the onset of filamentation. We also show that the suppression of filamentation observed for strongly perturbed equivalent barotropic evolutions, reported by Polvani *et al.*,[7,8] can also be understood in terms of the geometry of the streamfunction in the comoving frame.

In two dimensions, with $\nabla\cdot\mathbf{u} = 0$, the streamfunction ψ can be calculated from the vorticity distribution. With piecewise constant vorticity and

$$\nabla^2\psi_i = q, \quad \text{for } r \in D, \quad \nabla^2\psi_o = 0, \quad \text{for } r \notin D, \qquad (1)$$

where q is a constant and the velocities are functionals of the

0899-8213/89/020181-04$01.90

shape of the boundary ∂D of the region D. The points on ∂D are convected with the velocities $(u,v) = (\dot{x},\dot{y}) = (-\psi_y, \psi_x)$. This fact is the source for recent work with contour dynamics[9] and contour surgery.[10] In this Letter, D will be, initially, an unstably perturbed Kirchhoff ellipse.

First, consider finding the critical points for the corotating streamfunction of the unperturbed ellipse, whose angular velocity[11] is $\Omega = qab/(a+b)^2$. For convenience we take $q = 1$, $ab = 1$, and $\lambda \equiv b/a$ to be the ratio of the minor-to-major axis $(0<\lambda<1)$. The elliptic-Cartesian coordinate system conversion is

$$(x,y) = c(\cosh\rho\cos\vartheta, \sinh\rho\sin\vartheta),$$

where $c = (a^2-b^2)^{1/2} = (1-\lambda^2)/\lambda$. The ellipse is defined by the equation $\rho = \rho_0 = \tanh^{-1}\lambda$ and the inner and outer streamfunctions are, respectively,

$$\psi_i = \tfrac{1}{2}(1+\lambda)^{-1}(\lambda x^2 + y^2), \quad \text{for } \rho<\rho_0,$$

$$\psi_o = \tfrac{1}{2}\rho + \tfrac{1}{4}e^{-2\rho}\cos 2\vartheta, \quad \text{for } \rho>\rho_0.$$

The proper outer corotating streamfunction (see Fig. 1) is

$$\psi_c = \psi_o - \tfrac{1}{2}\Omega(x^2+y^2) = \psi_o - \tfrac{1}{4}\Omega c^2(\cosh 2\rho + \cos 2\vartheta),$$

and the hyperbolic critical points (S_1 and S_2 in Fig. 1) are obtained by solving

$$\partial_\rho \psi_c = 0 \quad \text{and} \quad \partial_\vartheta \psi_c = 0,$$

which yield, respectively,

$$\rho_c = \tfrac{1}{2}\log[(1+3\lambda)/(1-\lambda)] \quad \text{and} \quad \vartheta_c = 0,\pi.$$

Thus the ratio of the distance of the critical point from the origin along the x axis (x_c) to the major axis of the ellipse (a) is given by $(x_c/a) = (1+\lambda)^{3/2}/(1+3\lambda)^{1/2}$. For a circle ($\lambda\to 1$), $(x_c/a)\to\sqrt{2}$, and for a sheet ($\lambda\to 0$), $(x_c/a)\to 1$. One can conjecture that, in general, critical points may always be very close to contours on stationary states which have very high curvature. Near a hyperbolic point the curvature of the corotating streamline is very high, and for a stationary state the contour itself must be a streamline.

Incidentally, for a circle of radius R, it is easy to show that a harmonic perturbation of mode m has m critical points equispaced along a circle of radius

$$r_{c,m} = [m/(m-1)]^{1/2}R.$$

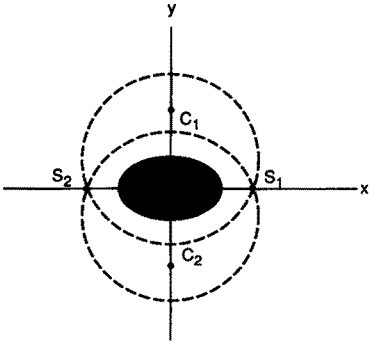

FIG. 1. The geometry of the corotating streamfunction of a Kirchhoff ellipse. The dotted lines are the separatrices, S_1 and S_2 are the hyperbolic (saddles) critical points, and C_1 and C_2 are the elliptic ones (centers).

Thus, for increasing m, they approach the vortex boundary. This simple result explains why the *limiting* rotating Euler V states[12] decrease their aspect ratio as m increases. Namely, one class of limiting V states arises when the critical points on the corotating streamfunction touch the vortex boundary, so that the boundary has a corner. This concept generalizes to the multilayer geostrophic context.[13] The above result also indicates that for localized Gaussian perturbations on a Rankine vortex, higher initial steepness leads to filamentation at shorter times, in accordance with the findings of Dritschel.[3] Finally, these considerations lead us to conjecture that, due to the inevitable presence of critical points, monopolar 2-D nonaxisymmetric vortex equilibria with a *smooth* (i.e., infinitely differentiable) vorticity distribution cannot exist.

Next we examine the linear stability and corresponding critical points of a perturbed ellipse. Let the total streamfunction be $\Psi = \psi + \varphi$, where φ is the perturbation. Following Love,[6] we expand the outer and inner perturbation streamfunction in harmonics,

$$\varphi_i = (\alpha_m/m)\cosh m\rho\sin m\vartheta + (\beta_m/m)\sinh m\rho\sin m\vartheta,$$

$$\varphi_o = (\alpha_m/m)\cosh m\rho_0\, e^{-m\rho}\cos m\vartheta + (\beta_m/m)\sinh m\rho_0\, e^{-m\rho}\sin m\vartheta,$$

with α_m and β_m functions of time alone and the perturbed boundary given by

$$\rho = \rho_v(\vartheta,t) = \rho_0 - h_0^2(\alpha_m\cos m\vartheta + \beta_m\sin m\vartheta),$$

where $h_0^{-2} = \lambda^{-1}\cos^2\vartheta^2 + \lambda\sin^2\vartheta$. Love[6] showed that α_m and β_m are related by a coupled harmonic system, for which the growth rates s are found from the dispersion relation

$$s^2 = \frac{1}{4}\left[\left(\frac{1-\lambda}{1+\lambda}\right)^{2m} - \left(\frac{2m\lambda}{(1+\lambda)^2}\right)^2\right].$$

With the initial conditions $\alpha_m = \epsilon$ and $\beta_m = 0$, we obtain

$$\rho_v(\vartheta,t) = \rho_0 + \epsilon\frac{\cosh st\cos m\vartheta + \mathscr{L}\sinh st\sin m\vartheta}{\lambda\cos 2\vartheta + (1/\lambda)\sin 2\vartheta}, \tag{2}$$

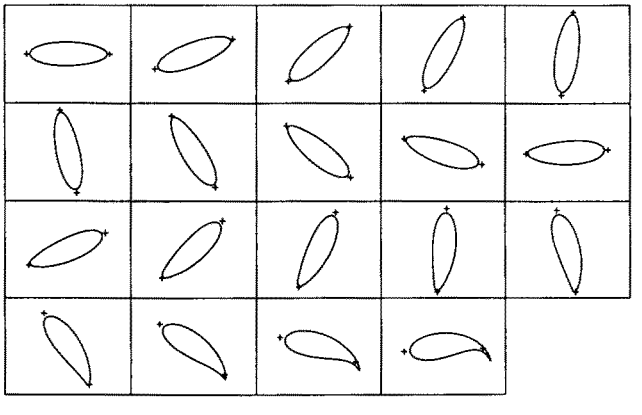

FIG. 2. The evolution of a $\lambda = 0.3$ Kirchhoff ellipse, initially perturbed with an unstable $m = 3$ Love mode of amplitude $\epsilon = 0.02$. The crosses indicate the positions of the hyperbolic critical points of the instantaneous corotating streamfunction. Time advances to the right and downward, and the frames shown correspond to $t = 0,2,4,6,\ldots,36$.

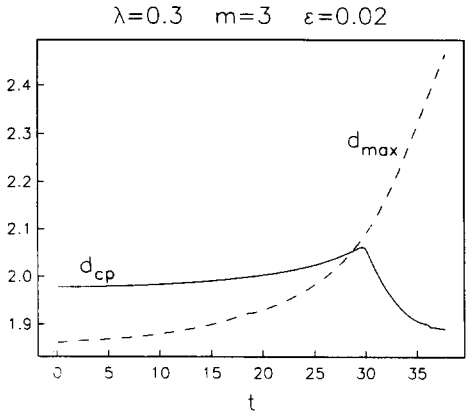

FIG. 3. The maximum distance from the contour to the origin (d_{max}) and the distance from the critical point S_1 to the origin (d_{cp}) versus time for the run of Fig. 2.

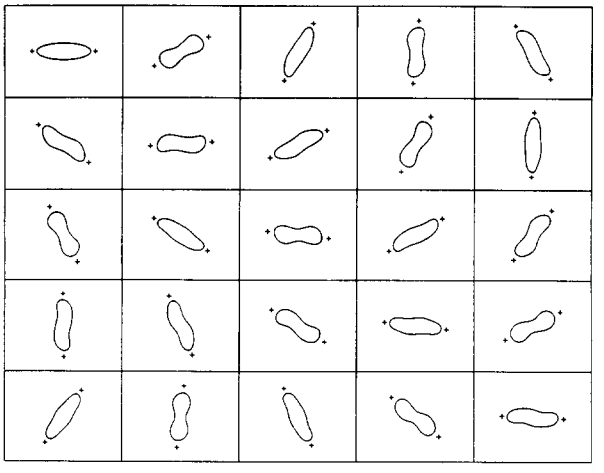

FIG. 4. The evolution of an initially unperturbed equivalent barotropic $\lambda = 0.3$ elliptical vortex at $\gamma = 3$. The time frames are $t = 0,40,80,\ldots,960$.

where $\mathscr{L} = e^{-m\rho_0}\cosh m\rho_0 - (m\lambda)/(1+\lambda)^2$. The perturbed critical points, located at $(P_c(t), \Theta_c(t))$, are found by solving

$$\partial_\rho \Psi_c(P_c,\Theta_c) = 0 \quad \text{and} \quad \partial_\vartheta \Psi_c(P_c,\Theta_c) = 0,$$

where $\Psi_c = \psi_c + \phi_o$ is the perturbed outer corotating streamfunction. If

$$P_c = P_c^{(0)} + \epsilon P_c^{(1)} + O(\epsilon^2),$$
$$\Theta_c = \Theta_c^{(0)} + \epsilon\Theta_c^{(1)} + O(\epsilon^2),$$

then we find that $P_c^{(0)} = \rho_c$, $\Theta_c^{(0)} = \vartheta_c$, and

$$P_c^{(1)} = \frac{\cosh m\rho_c \cos m\vartheta_c e^{-m\rho_c}}{(\Lambda - e^{-2\rho_c})}\cosh st, \tag{3a}$$

$$\Theta_c^{(1)} = \frac{\mathscr{L}\sinh m\rho_c \cos m\vartheta_c e^{-m\rho_c}}{(\Lambda - e^{-2\rho_c})}\cosh st, \tag{3b}$$

where $\Lambda = (1-\lambda)/(1+\lambda)$.

The linear estimate t_{CL}, for the time when the critical point coincides with the perturbed vortex boundary, is found by substituting (3a) and (3b) into (2):

$$t_{CL} \approx \frac{1}{s}\left[\log\left(\frac{\rho_c - \rho_0}{\epsilon}\right) - \log\left(\frac{1}{2\lambda} - \frac{\cosh m\rho_c e^{-2\rho_c}}{2(\Lambda\cosh 2\rho_c - e^{-2\rho_c})}\right)\right]. \tag{4}$$

The approximation in (4) arises from mixing the orders of the asymptotic expansion and omitting terms proportional to e^{-st}.

Figure 2 shows the contour dynamical evolution of a perturbed $\lambda = 0.3$ ellipse ($m = 3, \epsilon = 0.02$). The angular velocity necessary to determine a corotating streamfunction is obtained by fitting the entire contour to an ellipse at each time step[13] (this is not a unique procedure): the hyperbolic points are shown by crosses (+). The crossing is shown more precisely in the plot of d_{cp} and d_{max} vs t (Fig. 3), where d_{cp} is the distance of the relevant hyperbolic point (S_1) to the origin and d_{max} is the distance from the origin to the extreme point on the ellipse. The time of crossing, in Fig. 3, is $t_C \approx 28.5$, whereas from (4) we obtain $t_{CL} \approx 30.4$. The minimum value of the curvature along the contour becomes negative at $t \approx 27.8$; this corresponds to the appearance of an inflection point on the contour and, shortly afterward, the filament is seen to emerge. It should be noted that the increase of d_{cp} vs t for $t < 28$ is a property of the linear theory [cf. Eq. (3a)] and is due to the outward motion of the contour. A similar comparison for a $\lambda = 0.2$ perturbed ellipse ($m = 4, \epsilon = 0.02$) yields a crossover at $t_C \approx 14.3$, an estimate from (4) of $t_{CL} \approx 17.5$, and the appearance of negative curvatures at $t \approx 14.0$.

An examination of equivalent barotropic dynamics[7,8] shows a similar phenomenon. If (1) is replaced by

$$(\nabla^2 - \gamma^2)\psi_i = \Pi, \quad \text{for } r \in D$$

and

$$(\nabla^2 - \gamma^2)\psi_o = 0, \quad \text{for } r \notin D,$$

with Π constant and $(\partial_t + \mathbf{u}\cdot\nabla)(\nabla^2 - \gamma^2)\psi_{i,o} = 0$, we obtain the evolution and critical points shown in Fig. 4 for an initially unperturbed $\lambda = 0.3$ ellipse at $\gamma = 3$. Although the vortex undergoes nonlinear oscillations, no filamentation or crossings are observed, and the critical points never come into contact with the contour.

ACKNOWLEDGMENTS

The authors wish to express their gratitude to Anne-Marie Michael who graciously expended much effort to produce a legible manuscript from a virtually unreadable original, and to Dr. D. G. Dritschel for providing them with his latest results before publication.

This work was funded in part by the Office of Naval Research under Contracts No. N00014-85-K-0024 to NJZ and No. N00014-86-K-0325 to GRF.

[a] Present address: Department of Mathematics, Room 2-339, Massachusetts Institute of Technology, Cambridge, Massachusetts 02139.
[b] Permanent address: Department of Mechanical and Aerospace Engineering, Rutgers University, Piscataway, New Jersey 08855-0909.

[1]M. V. Melander, J. C. McWilliams, and N. J. Zabusky, J. Fluid Mech. **178**, 137 (1987).
[2]G. S. Deem and N. J. Zabusky, Phys. Rev. Lett. **40**, 859 (1978).
[3]D. Dritschel, J. Fluid Mech. **194**, 511 (1988).
[4]D. I. Pullin, J. Fluid Mech. **108**, 401 (1981).
[5]D. I. Pullin, P. A. Jacobs, R. H. J. Grimshaw, and P. G. Saffman (private communication).
[6]A. E. H. Love, Proc. London Math. Soc. **35**, 18 (1893).
[7]L. M. Polvani, N. J. Zabusky, and G. R. Flierl, Fluid Dyn. Res. **3**, 422 (1988).
[8]L. M. Polvani, N. J. Zabusky, and G. R. Flierl, submitted to J. Fluid Mech.
[9]N. J. Zabusky, M. H. Hughes, and K. V. Roberts, J. Comput. Phys. **30**, 96 (1979).
[10]D. G. Dritschel, J. Comput. Phys. **77**, 240 (1988).
[11]Sir H. Lamb, *Hydrodynamics* (Dover, New York, 1945), 6th ed., p. 159.
[12]H. M. Wu, E. A. Overman, and N. J. Zabusky, J. Comput. Phys. **53**, 42 (1984).
[13]L. M. Polvani, Ph.D. thesis, Massachusetts Institute of Technology, 1988.

Space-time correlations in turbulence: Kinematical versus dynamical effects

Victor Yakhot, Steven A. Orszag, and Zhen-Su She
Applied and Computational Mathematics Program, Princeton University, Princeton, New Jersey 08544

(Received 6 October 1988; 17 November 1988)

Space and time correlation functions in a randomly stirred turbulent fluid are evaluated to lowest order of the ϵ expansion in the renormalization group theory of turbulence. It is shown that wavenumber and frequency energy spectra differ substantially since random sweeping effects on the small eddies by large-scale eddies do not contribute to the decorrelation in the RNG theory.

The strong nonlinearity of the Navier–Stokes equations at high Reynolds numbers makes theoretical analysis of fully developed hydrodynamic turbulence difficult and excludes the usual perturbative treatments. From the physical point of view, the difficulty stems from the fact that, at large Reynolds numbers, a very large range of scales is excited; the interaction between these scales is still poorly understood physically. One of the important questions is how the most energetically excited scales (at the so-called integral scale) interact with much smaller inertial-range scales, and how the interaction influences Eulerian experimental measurements. The random Galilean invariance principle introduced by Kraichnan[1] postulates that the small-scale motions undergo purely kinematic advection by large-scale eddies, which causes decorrelation by a sweeping effect directly measurable in the Eulerian frame. Since the large-scale eddies have the greatest excitation, this sweeping effect leads to a shorter correlation time in an Eulerian frame than that in a Lagrangian frame, where the correlation time is determined mainly by the local eddy turnover time. However, this relationship between Eulerian and Lagrangian correlation times does not hold uniformly. In fact, it is easy to construct examples of flow systems[2–4] in which the Lagrangian correlation time is smaller than the Eulerian one.

To illustrate the decay of velocity correlations through sweeping effects, consider the Fourier-space correlation,

$$G(k,t) = \langle v(k,0)v(k,t)\rangle = \langle v^2(k,0)e^{ikVt - ak^z t}\rangle_{v,V}, \qquad (1)$$

where V is the random sweeping velocity introduced by the large scales on the small ones. The term proportional to k^z takes into account the dynamics of interactions of the modes $\mathbf{v}(\mathbf{k})$ and $\mathbf{v}(\mathbf{q})$ with $k \simeq q$. The exponent z must be determined by appropriate dynamical theory. The average in (1) is done over both small- and large-scale fields, $\mathbf{v}(\mathbf{k},0)$ and $\mathbf{V}$, respectively. If it is assumed that *the small and large scales are decorrelated* and that the large-scale field $\mathbf{V}$ is Gaussian, then

$$G \sim \phi(k)e^{-ak^z t}\langle e^{ikVt}\rangle_V \sim \phi(k)e^{-k^2V^2t^2 - ak^z t}, \qquad (2)$$

where $\phi(k) = \langle v^2(k,0)\rangle_v$. As $t \to \infty$, the decay of the correlation function G is dominated by dephasing caused by random sweeping effects.

This kinematic sweeping effect also appears in the form of infrared divergences in the field-theoretical diagrammatic perturbation description of turbulence. Partial resummations like the direct interaction approximation (DIA) suffer from this divergence. The primary motivation for the Lagrangian modifications of DIA was the elimination of this infrared divergence.[5,6]

In this Letter, we use the renormalization group (RNG) approach developed by us[7–9] for the analysis of space-time correlations in homogeneous turbulence. The RNG analysis has already produced good quantitative predictions for inertial-range dynamics. The RNG analysis is based on the correspondence principle[7] that general, fully developed turbulent flow subject to initial and boundary conditions is equivalent in *the inertial range* to flow governed by the Navier–Stokes equations driven by the Gaussian random force, defined by the three-dimensional correlation function

$$\langle f_i(\mathbf{k},\omega)f_j(\mathbf{k}',\omega')\rangle = (2\pi)^4 2D_0 k^{1-\epsilon}P_{ij}(\mathbf{k})\delta(\mathbf{k}+\mathbf{k}')\delta(\omega+\omega'), \qquad (3)$$

where $P_{ij}(\mathbf{k}) = \delta_{ij} - k_i k_j/k^2$, and $\epsilon = 4 - \mu/2$ with $0 < \mu < 10$. At the present time, the correspondence principle is a

 0899-8213/89/020184-03$01.90